Electronic Supplementary Material (ESI) for Chemical Communications.
This journal is © The Royal Society of Chemistry 2022

Supporting Information

Multiple pH Waves Generated Electrochemically and Propagated from an Electrode Surface

Ilya Sterin,[§] Anna Tverdokhlebova,[§] Evgeny Katz,* Oleh Smutok*

Department of Chemistry and Biomolecular Science, Clarkson University, Potsdam, NY 13699-5810, USA.
* Corresponding authors: E-mails: osmutok@clarkson.edu (OS); ekatz@clarkson.edu (EK)
[§] The authors contributed equally

Table of contents

Chemicals

Sodium ascorbate (Sigma Aldrich), sodium phosphate dibasic heptahydrate (Thermo Fisher Scientific), sodium phosphate monobasic anhydrous (Thermo Fisher Scientific), sodium sulfate (Thermo Fisher Scientific), hydrogen peroxide (Thermo Fisher Scientific), hydrochloric acid (Thermo Fisher Scientific), sodium hydroxide (Thermo Fisher Scientific), dimethyl sulfoxide (Thermo Fisher Scientific), and ethyl alcohol anhydrous (Pharmco Aaper) were used as received without further purification. The pH-sensitive fluorescent dyes were synthesized[1] according to the procedures reported in literature: 3,4'-dihydroxy-3',5'-*bis*-(dimethylaminomethyl)flavone (FAM345)[2] and rhodamine-6-aniline (R6H).[3] All experiments were carried out using ultrapure water (18.2 MΩ·cm; Barnstead NANOpure Diamond).

Instrumentation

Fluorescent images were obtained with Leica TCS SP5 II Tandem Scanning Confocal and Multiphoton Microscope. Processing of images for pH estimation was done with Adobe Photoshop software. Fluorescence measurements were performed in 96-well microplate using a SpectraMax MiniMax 300 Imaging Cytometer (Molecular devices) and SoftMax Pro 6 software. A Mettler Toledo S20 SevenEasy pH meter was used to measure pH of the solutions. Cyclic voltammetry and constant-potential electrolysis experiments were performed using an electrochemical workstation (ECO Chemie Autolab PASTAT 10) and GPES 4.9 (General Purpose Electrochemical System) software. The potentials were measured using a BASi Ag|AgCl|KCl, 3 M, reference electrode.

Electrochemical experiments

Optimal solution for the system was composed of 12.5 µM FAM345 dye, 15 µM R6H dye, 6 mM sodium ascorbate, 4 mM H_2O_2, O_2 in equilibrium with air, 100 mM Na_2SO_4 in 2 mM phosphate buffer, pH 7.0. Petri dish was used to improvise an electrochemical cell. A part of the Petri dish was separated with a plasticine barrier to form the electrochemical cell (see Figure SI4). A graphite flat electrode (GFE), 3 cm^2 geometrical surface area, was used as the working electrode. A GFE electrode was polished with 1500 Grit sandpaper (3 M Wettodry), sonicated in ethanol for 3 minutes, and finally polished with a KimTech kimwipe (Kimberly-Clark Professional) to prepare the electrode surface for experiments. A similar electrode was used as a counter electrode. The potentials were measured using a BASi Ag|AgCl|KCl, 3 M, reference electrode. Potential scan rate for all experiments was 10 mV/s. Confocal fluorescence measurements were performed during the constant-potential electrolysis (see Figure SI3 for the experimental setup). Potential switch programs used to achieve triple pH waves are shown in Table 1.

Table 1. The optimized experimental conditions for creation of triple pH waves

Triple wave type	Potential applied, V	Time interval, s
Acidic-basic-acidic	+0.6	90
	-0.8	35
	+0.6	10
Basic-acidic-basic	-0.8	65
	+0.6	15
	-0.8	15

Dependence of dye's fluorescence on bulk pH

To check the dependence of dyes' fluorescence intensity on the solution pH, 0.5 mL solutions were prepared in 2 mM phosphate buffer, which contained 12.5 µM FAM345 or/and 15 µM R6H, 4 mM H_2O_2, O_2 in equilibrium with air, 6 mM sodium ascorbate, 100 mM Na_2SO_4. Then, fluorescence was assessed on the confocal microscope (CFM), and on the Imaging Cytometer (microplate reader).

For FAM345 pH was varied between 7 and 11. For R6H pH was varied between 3 and 7. The pH step in both experiments was 1 pH unit.

1) Settings on microplate reader:
- FAM345: λ_{ex} 405 nm, emission recorded between 470 and 550 nm. Emission maximum is observed @ 530 nm.
- R6H: λ_{ex} 540 nm, emission recorded between 565 and 605 nm. Emission maximum is observed @ 575 nm.

2) Settings on confocal microscope:
- FAM345: λ_{ex} 405 nm, emission recorded between 470 and 610 nm, gain 920.
- R6H: λ_{ex} 561 nm, emission recorded between 570 and 630 nm, gain 790.
- Magnification 10×

Processing of confocal fluorescent microscope images for the local (interfacial) pH estimation

The brightness of an image was assessed as a mean gray value, that was calculated using an analysis tool in Adobe Photoshop (namely, selecting Image → Analysis → Record Measurements). For evaluation of pH distribution, a band perpendicular to the electrode surface was selected, which was then divided in equal parts, and in each part the mean gray value was calculated. The cut-offs were set by visual perception using software of confocal microscope which automatically showed the layer thickness.

Concentration dependence of the pH layer formation

The experiments were performed with different concentrations of H_2O_2 and ascorbate (note that the O_2 concentration was always the same under equilibrium with air), then always resulting in the formation of layers with different pH values. The results reported in the paper were performed using experimentally optimized concentrations of the reactants which allowed the best visualization of the pH layers in the presence of fluorescent dyes. The optimized solution composition was: O_2 (in equilibrium with air), 4 mM H_2O_2, 6 mM sodium ascorbate, 12.5 µM FAM345, 15 µM R6H, and 100 mM Na_2SO_4 in 2 mM phosphate buffer, pH 7.0.

Justification of the use of H_2O_2 as an additional oxidizer along with O_2

In some recent publications were used only O_2 as the redox species which reduction accompanied with H^+ consumption resulted in pH increase (see for example refs. 4, 19 in the paper). This was sufficient for formation of single pH layers with the increased pH values. When the present project was started, we have tried to use O_2 as the reducible species, following our previous results. However, soon we found experimentally that formation of multiple pH layers requires higher concentration of redox species. Since it was not easy to increase O_2 concentration in the solution (otherwise we had to use a closed electrochemical cell which was not easy to accommodate in the optical system of the confocal microscope), we decided to add another reductant, which was H_2O_2. Notably, H_2O_2 is an intermediate product of the O_2 electrochemical reduction, thus, its presence does not change too much the mechanism of the process. The use of H_2O_2 allowed easy variation and optimization of its concentration. Actually, the experiments could be performed using only H_2O_2 without oxygen, however, this would require a closed electrochemical cell with removed O_2, thus complicating the experimental setup.

References

1 P. Bollella, A. Melman, E. Katz**,** *ChemElectroChem* 2021, **8**, 3923-3935.

2 M. S. Frasinyuk, A. V. Turov, V. P. Khilya, *Chem. Heterocycl. Compd.* 1998, **34**, 923–928.

3 W. L. Czaplyski, G. E. Purnell, C. A. Roberts, R. M. Allred, E. J. Harbron, *Org. Biomol. Chem.* 2014, **12**, 526–533.

Additional Figures

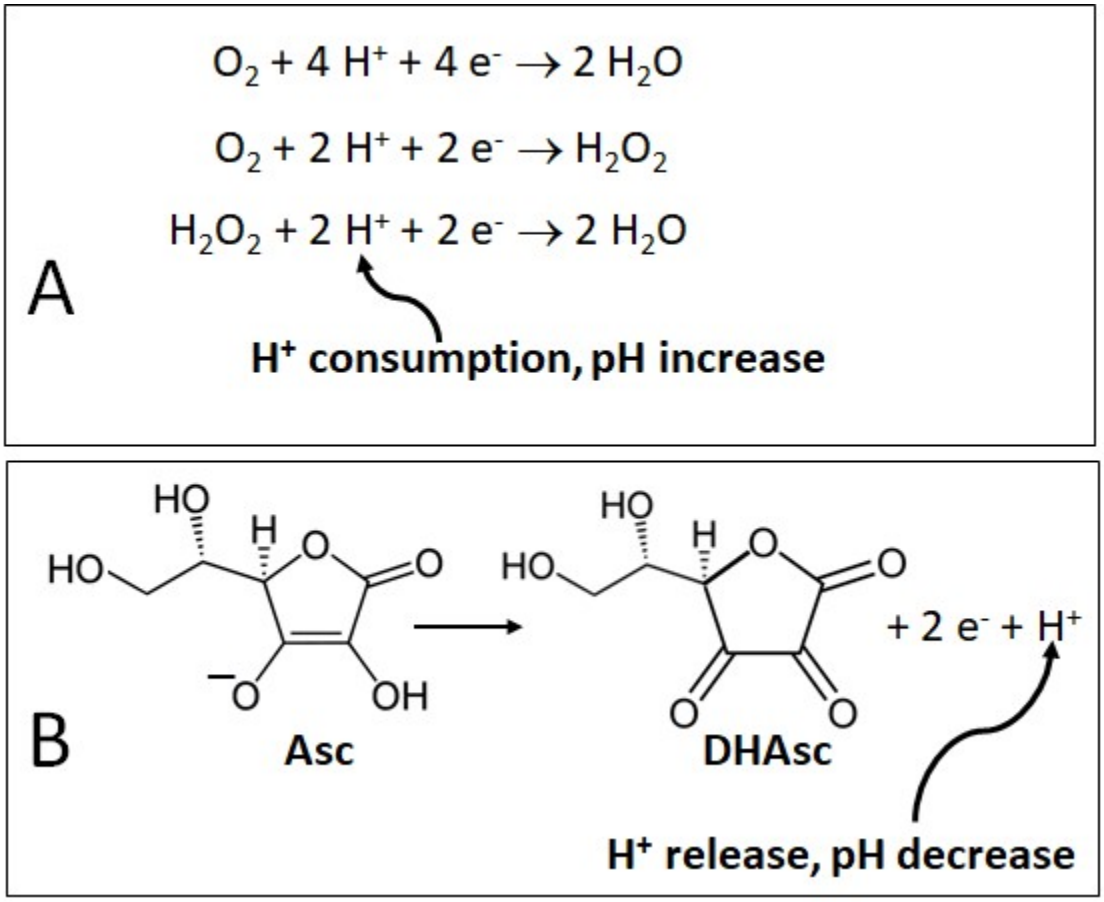

Figure SI1. (A) Electrochemical reduction of O_2 and H_2O_2 resulting in H^+ ion consumption and local (interfacial) pH increase. (B) Electrochemical oxidation of ascorbate (Asc) producing dehydroascorbate (DHAsc) resulting in H^+ ion release and local (interfacial) pH decrease.

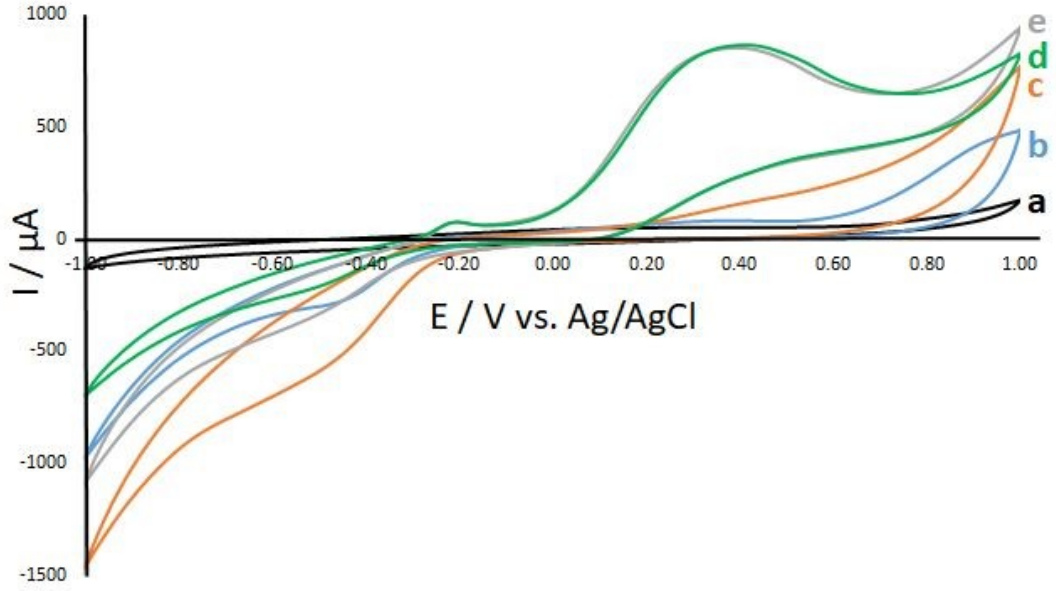

Figure SI2. Cyclic voltammograms of solutions with different compositions: (a) the background solution composed of 2 mM phosphate buffer, pH 7.0, under Ar (oxygen was removed by Ar bubbling through the solution at least 40 min); (b) the background solution composed of 2 mM phosphate buffer, pH 7.0, under air (oxygen was present in the solution under equilibrium with air); (c) 4 mM H_2O_2 was added to the background solution in the presence of O_2; (d) 6 mM sodium ascorbate was added to the background solution in the presence of O_2; (e) 6 mM sodium ascorbate and 4 mM H_2O_2 were added to the background solution in the presence of O_2. Potential scan rate 10 mV/s.

Comments:

a) All cyclic voltammetry experiments were performed with 12.5 µM FAM345 dye and 15 µM R6H dye added to the background solution to exclude the possibility of their participation in the redox reactions. Note that the cyclic voltammogram of the background solution in the absence of O_2 (under Ar) doesn't show any waves which may originate from the fluorescent dyes present in the solution (curve a).

b) Note that the anodic peaks at ca. 0.35 V (curves d and e) corresponding to electrochemical ascorbate oxidation are not affected by the presence of H_2O_2, thus showing no chemical ascorbate oxidation by H_2O_2.

c) Note significant increase of the cathodic current at ca. -0.5 V in the presence of H_2O_2 compared with the solution containing O_2 only. Thus, the reduction of H_2O_2 significantly contributes to the local pH increase.

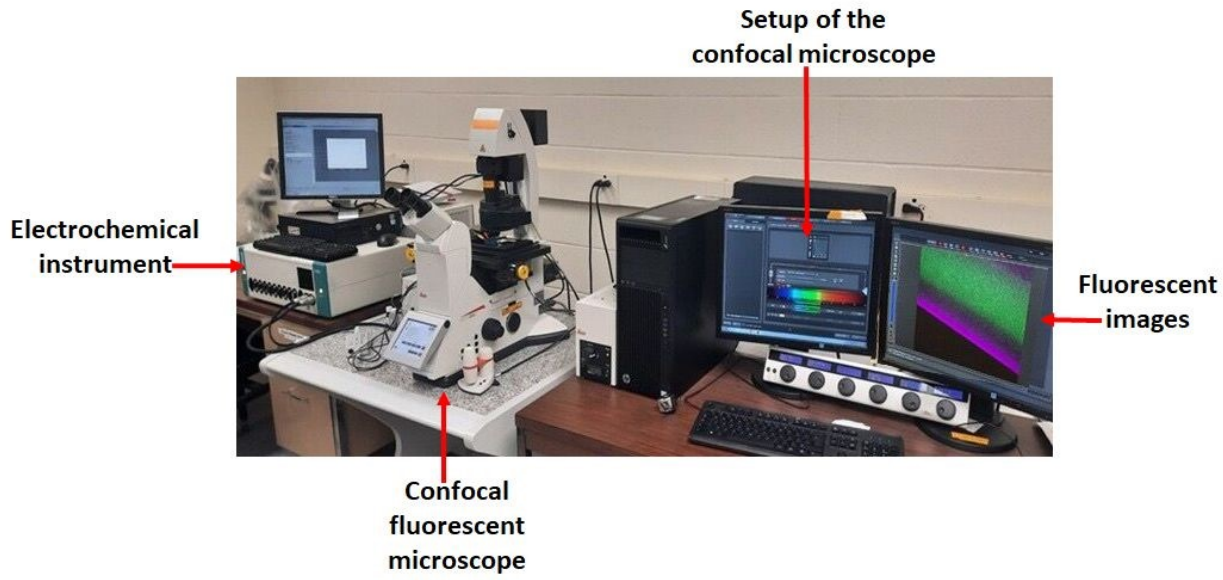

Figure SI3. The experimental setup including the confocal fluorescent microscope and the electrochemical instrument.

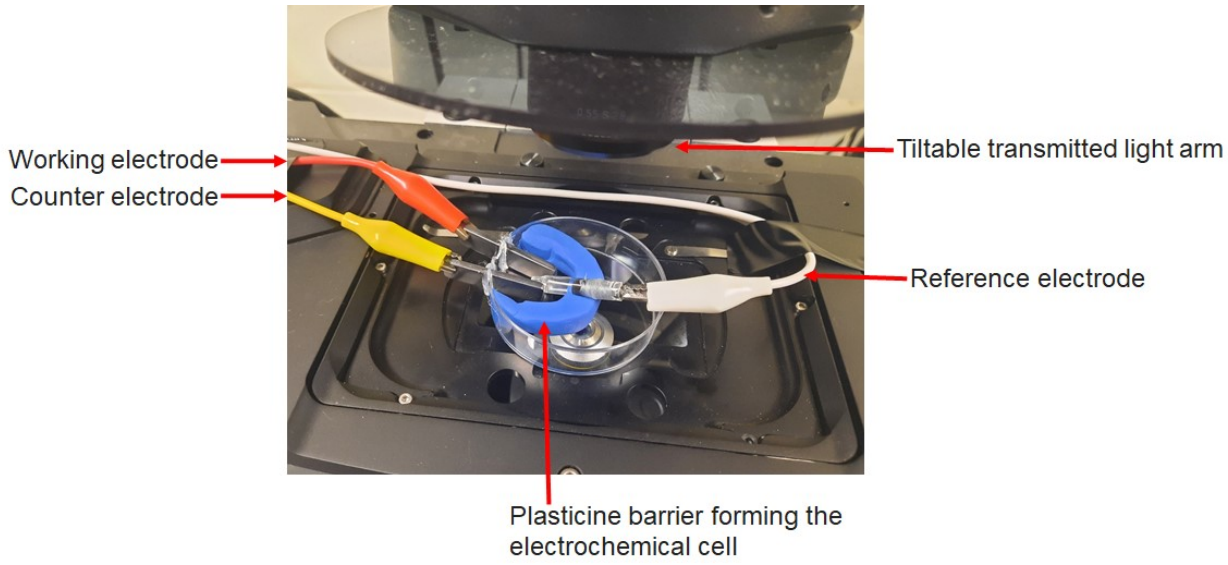

Figure SI4. The experimental setup; close view on the electrochemical cell.

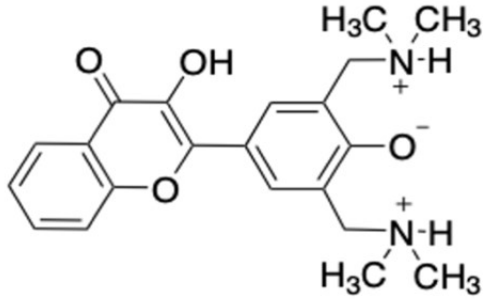

FAM345 dye (green fluorescence)

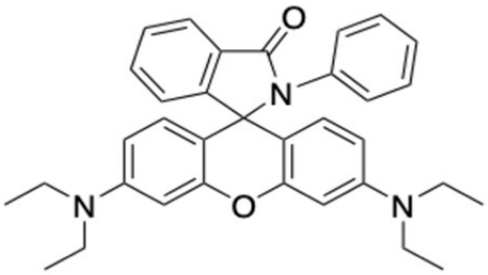

R6H dye (pink fluorescence)

Figure SI5. pH-Dependent fluorescent dyes used in the study.

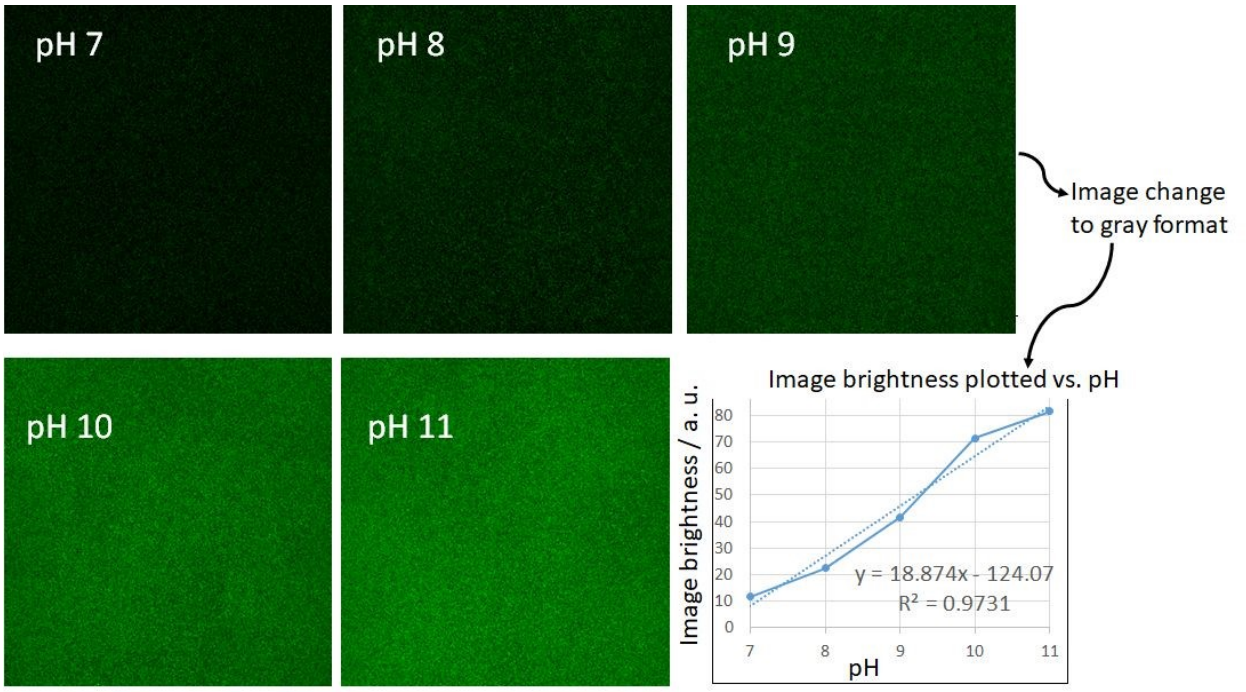

Figure SI6. Colored (green) images: Confocal fluorescent microscopy images of FAM345 dye obtained at different bulk pH values. Solution composition: 12.5 µM FAM345 dye, 6 mM sodium ascorbate, 4 mM H_2O_2, O_2 in equilibrium with air, 100 mM Na_2SO_4 in 2 mM phosphate buffer pH 7÷11. The plot shows dependence of the FAM345 fluorescence intensity on the bulk pH values (based on images' brightness).

How the images were processed: Confocal images of FAM345 dye taken at different pH values were processed through Adobe Photoshop software to relate color intensity with pH. The brightness of an image was assessed as a mean gray value, that was calculated using a software analysis tool (namely, selecting Image → Analysis → Record Measurements). This calibration was later used to quantify pH in images obtained from electrochemical experiments.

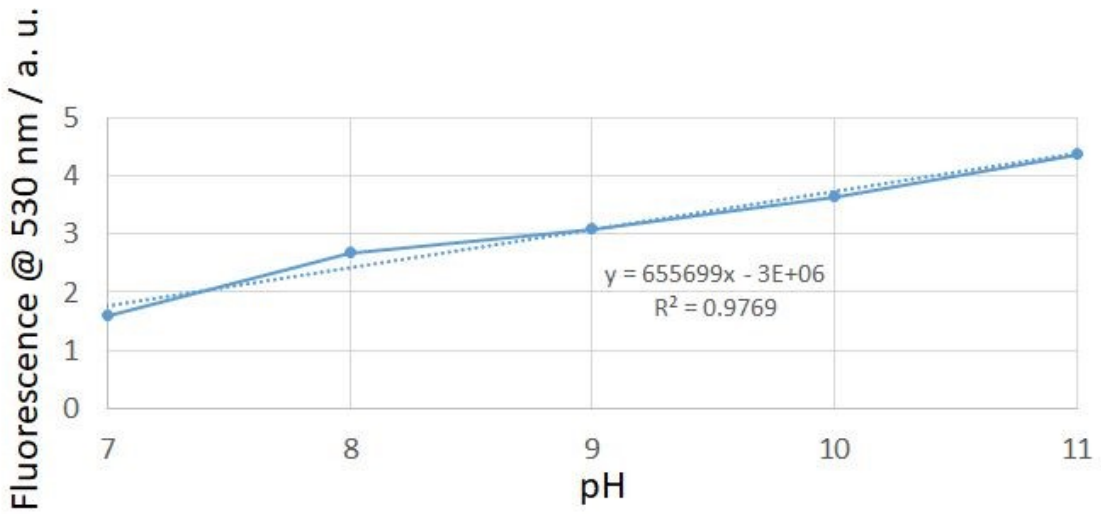

Figure SI7. Dependence of FAM345 fluorescence intensity on the bulk pH values (calibration based on fluorescence intensity). The fluorescence was measured in the bulk solution with a fluorimeter.

The dependence of FAM345 dye fluorescence on different bulk pH values was confirmed with two instruments: confocal microscope (see Figure SI6) and microplate fluorescence reader (imaging cytometer) (the present calibration plot).

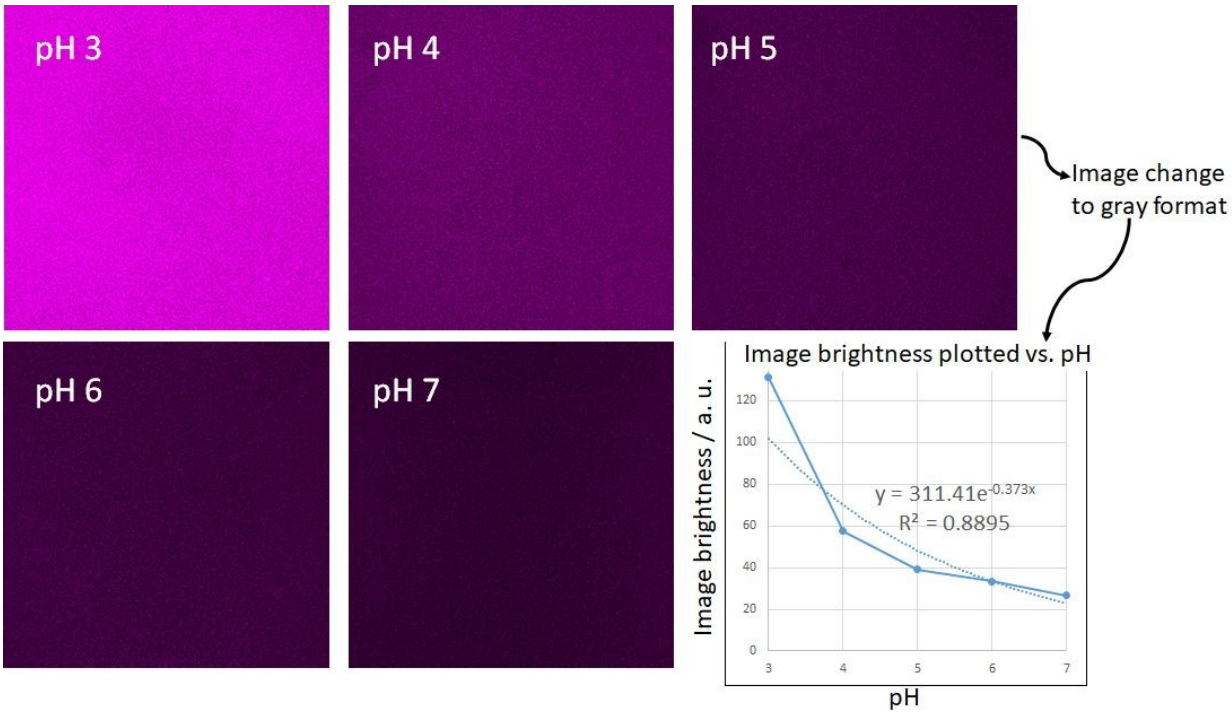

Figure SI8. Colored (pink) images: Confocal fluorescent microscopy images of R6H dye obtained at different bulk pH values. Solution composition: 15 µM R6H dye, 6 mM sodium ascorbate, 4 mM H_2O_2, O_2 in equilibrium with air, 100 mM Na_2SO_4 in 2 mM phosphate buffer pH 3÷7. The plot shows dependence of the R6H fluorescence intensity on the bulk pH values (based on images' brightness).

How the images were processed: Confocal images of R6H dye taken at different pH values were processed through Adobe Photoshop software to relate color intensity with pH. The brightness of an image was assessed as a mean gray value, that was calculated using a software analysis tool (namely, selecting Image → Analysis → Record Measurements). This calibration was later used to quantify pH in images obtained from electrochemical experiment.

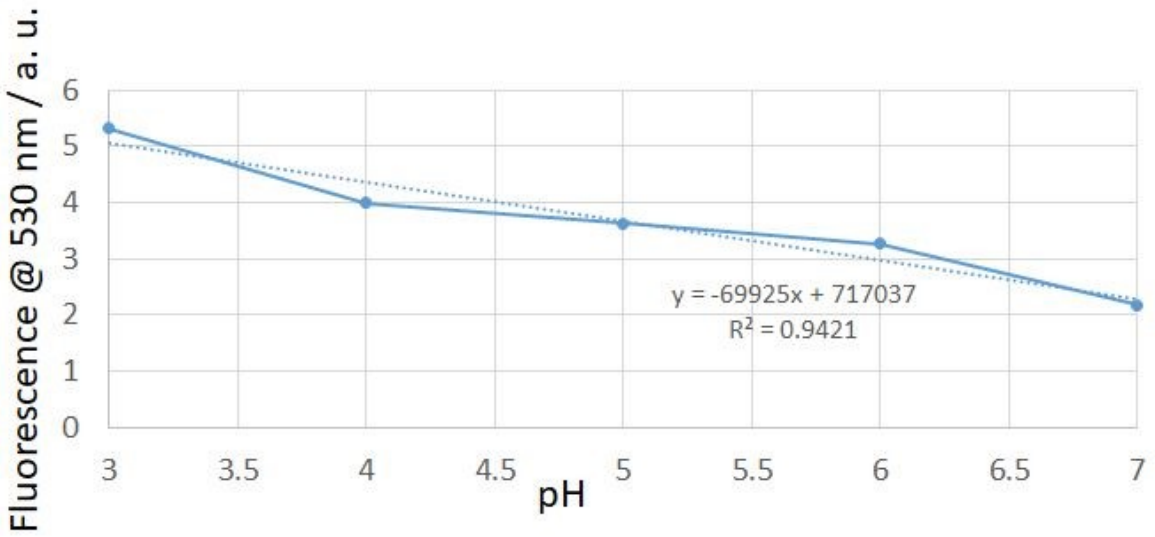

Figure SI9. Dependence of R6H fluorescence intensity on the bulk pH values (calibration based on fluorescence intensity). The fluorescence was measured in the bulk solution with a fluorimeter.

The dependence of R6H dye fluorescence on different bulk pH values was confirmed with two instruments: confocal microscope (see Figure SI8) and microplate fluorescence reader (imaging cytometer) (the present calibration plot).

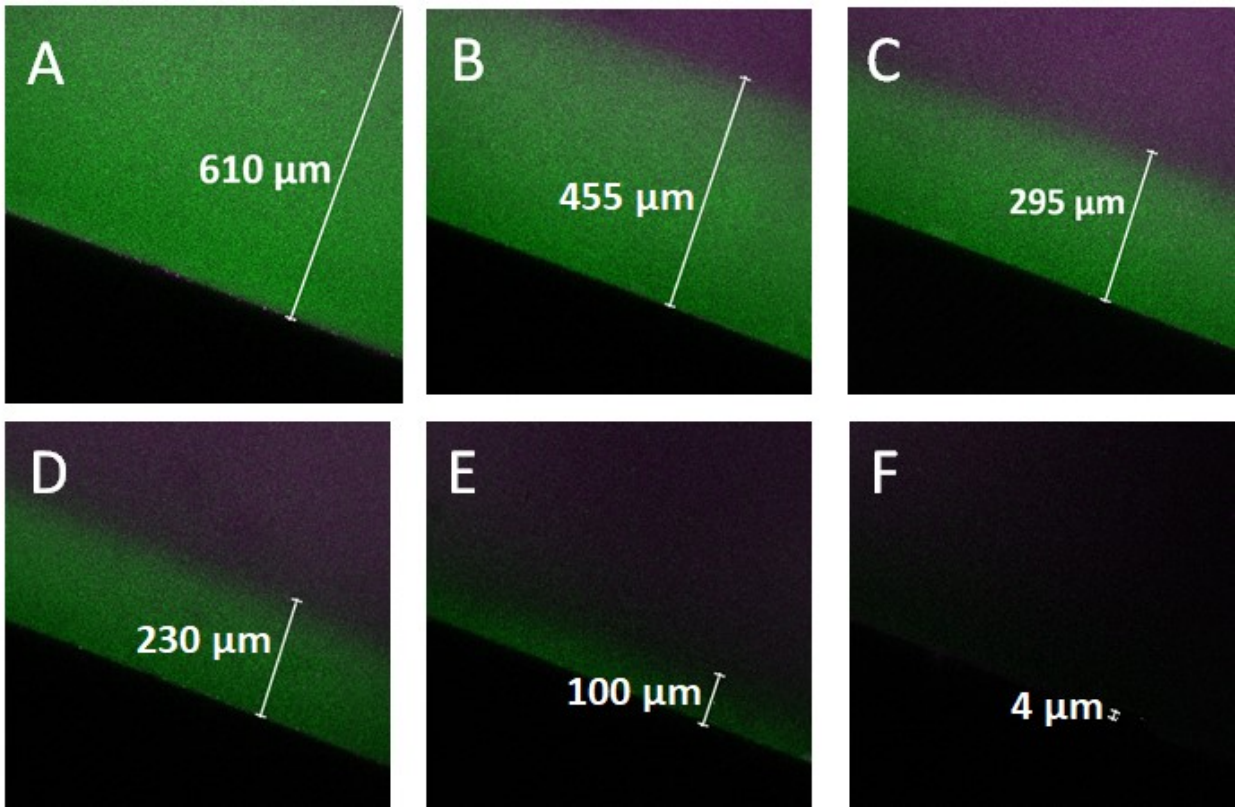

Figure SI10. Effect of buffer capacity on the propagation of local pH front. Phosphate buffer, pH 7.0, concentrations: (A) 1 mM, (B) 2 mM, (C) 4 mM, (D) 6 mM, (E) 8 mM, (F) 10 mM. The electrolysis corresponding to O_2 electrochemical reduction (O_2 was dissolved in equilibrium with air) was performed at -0.8 V (vs. Ag/AgCl reference). The green fluorescence was produced by the FAM345 dye (10 µM). The confocal microscope images were taken 50 s after application of -0.8 V potential. Note significant decrease of the pH change propagation upon the buffer concentration increase.

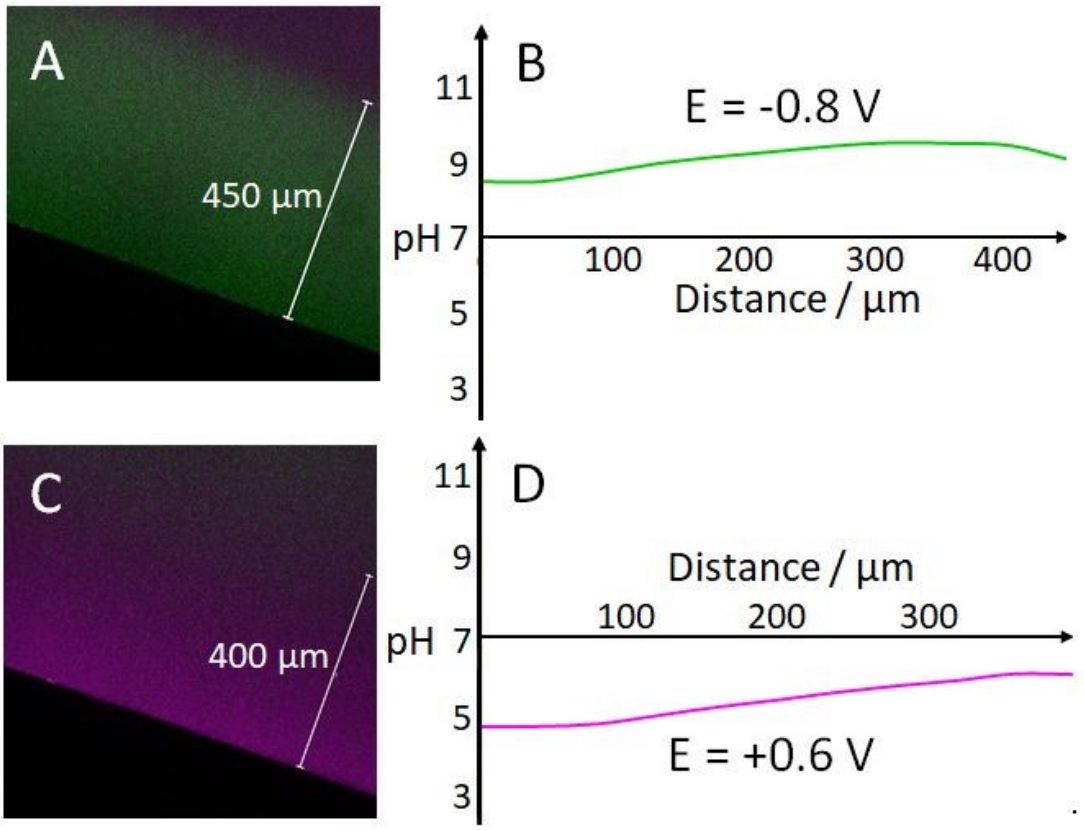

Figure SI11. pH-Distribution within the solution layers (single layer formation). (A) A confocal fluorescence image of a basic layer produced electrochemically upon O_2 and H_2O_2 reduction at the potential -0.8 V. (B) pH-Distribution within the layer shown in (A). (C) A confocal fluorescence image of an acidic layer produced electrochemically upon ascorbate oxidation at the potential +0.6 V. (D) pH-Distribution within the layer shown in (C). The solution composition: O_2 (in equilibrium with air), 4 mM H_2O_2, 6 mM sodium ascorbate, 12.5 µM FAM345, 15 µM R6H, and 100 mM Na_2SO_4 in 2 mM phosphate buffer, pH 7.0. The images were taken 70 s after the potential application.

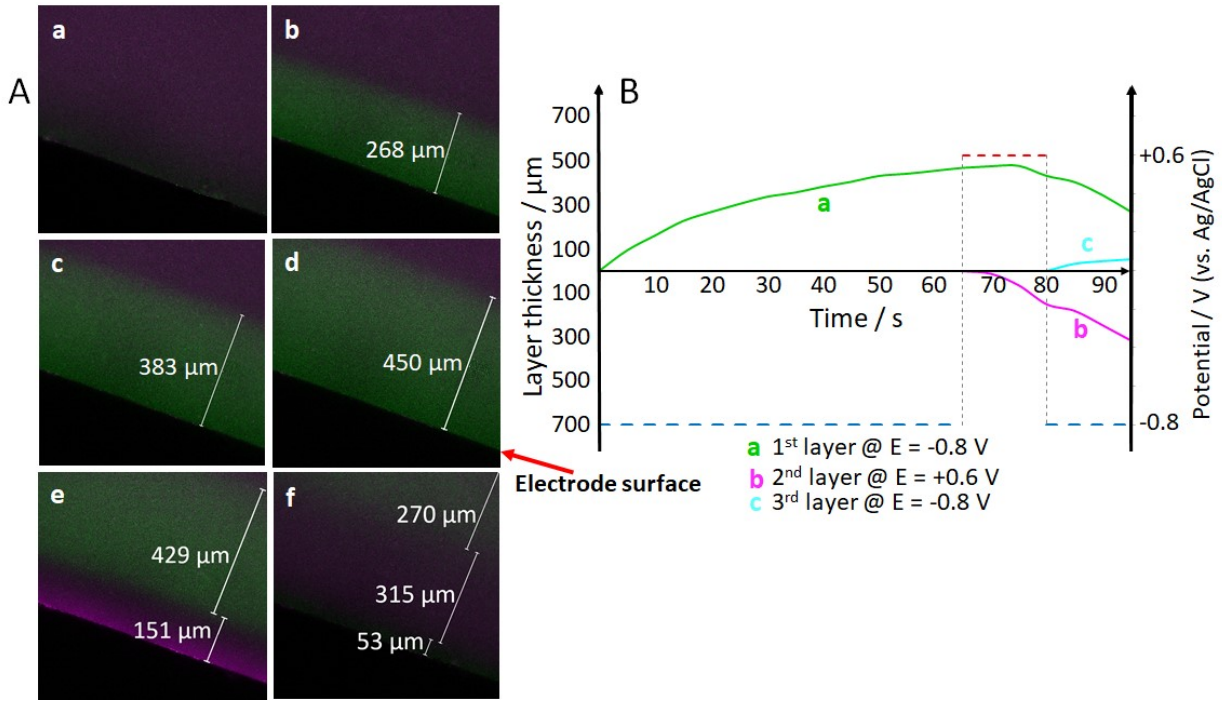

Figure SI12. pH-Waves (basic-acidic-basic) propagating from the electrode surface upon reversible switching of the potential applied on the electrode. The experiment is similar to one shown in Figure 2 in the paper, but with the potential switch in a different order. An animated image showing transformations of the layers with different pH values is available in the Supporting Information (see Image2). (A) Confocal fluorescence images of the interface obtained at different time intervals: (a) 0 s, (b) 20 s, (c) 40 s, (d) 60 s, (e) 80 s, (f) 95 s. The thickness of the solution layers with different pH values is shown in the images. (B) Changes in the thickness of the solution layers with different pH values in time. Potential -0.8 V was applied at time 0 s, then switched to +0.6 V at time 65 s, and then returned back to -0.8 V at time 80 s. The potential of -0.8 V resulted in reduction of O_2 and H_2O_2 leading to the formation of a basic layer (increased pH) at the electrode layer. The potential of +0.6 V resulted in ascorbate oxidation leading to the formation of an acidic layer (decreased pH) at the electrode surface. The potential of -0.8 V reapplied on the electrode resulted in the formation of another basic layer (increased pH) at the electrode surface. The solution composition: O_2 (in equilibrium with air), 4 mM H_2O_2, 6 mM sodium ascorbate, 12.5 µM FAM345, 15 µM R6H, and 100 mM Na_2SO_4 in 2 mM phosphate buffer, pH 7.0.

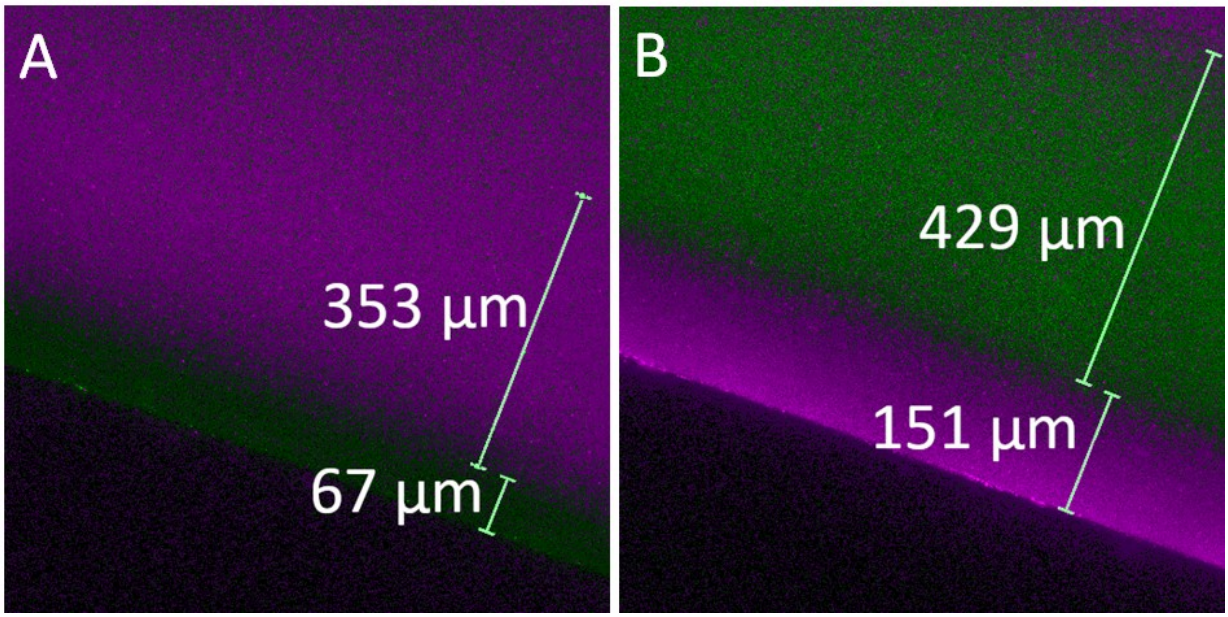

Figure SI13. The computer-processed images shown in Figures 2A,d and 3C in the paper. These example images have artificially increased contrast of green and pink colors corresponding to the layers with different pH values. The processing was done in a software called "Gimp" (GNU Image Manipulation Program). Actions on the tool bar were: Colors → Hue-Chroma → in the open window set Chroma bar on 75. Note that the artificial computer-processed image has slightly different numbers for the layer thickness, compared to the original image produced by the confocal microscope. Note that all other confocal fluorescent images shown in the paper and in ESI were not computer-processed and appear as obtained in the experiments.

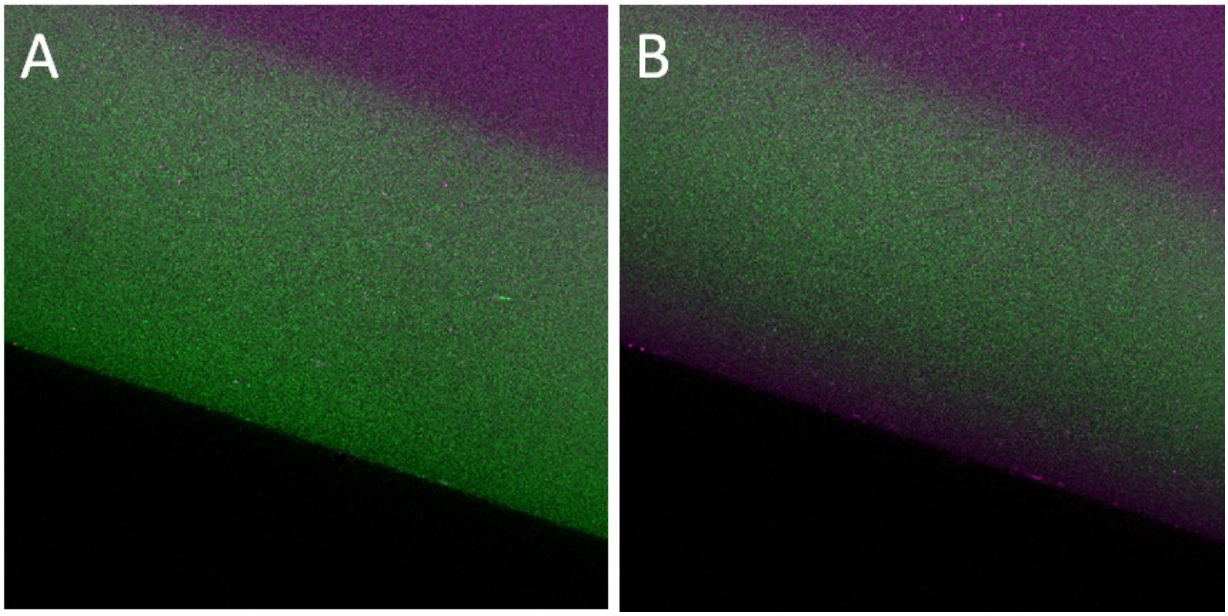

Figure SI14. Confocal fluorescent images obtained with different concentrations of the redox species. The solution composition: O_2 (in equilibrium with air), 1 mM sodium ascorbate, 12.5 µM FAM345, 15 µM R6H, and 100 mM Na_2SO_4 in 2 mM phosphate buffer, pH 7.0. Potential program: -0.8 V (formation of basic layer) followed by 0.6 V (formation of acidic layer). The images were taken at 210 s and 250 s (A and B, respectively).

Comments:

As it can be seen, 1 mM ascorbate is not enough for clear visualization of the acidic layer that follows the basic layer. This required the use of higher ascorbate concentration, but such high concentration impaired visualization of basic layer (not shown here). The pH-layer formation was improved upon using experimentally optimized concentrations of ascorbate and H_2O_2 (see all other fluorescent images in the paper and SI).